Differential regulation of synaptic $GABA_A$ receptors by cAMP-dependent protein kinase in mouse cerebellar and olfactory bulb neurones

Zoltan Nusser, Werner Sieghart* and Istvan Mody

*Department of Neurology, UCLA School of Medicine, 710 Westwood Plaza, Los Angeles, CA 90095-1769, USA and *Section of Biochemical Psychiatry, University Clinic for Psychiatry, Wahringer-Gurtel 18-20, A-1090 Vienna, Austria*

(Received 25 June 1999; accepted after revision 24 September 1999)

1. It has been demonstrated that the regulation of recombinant $GABA_A$ receptors by phosphorylation depends on the subunit composition. Here we studied the regulation of synaptic $GABA_A$ receptor function by cAMP-dependent protein kinase (PKA) in neurones expressing distinct receptor subtypes.

2. Light microscopic immunocytochemistry revealed that granule cells of the olfactory bulb express only the $\beta3$ as the β subunit variant, whereas cerebellar stellate and basket cells express only the $\beta2$ as the β subunit.

3. In cerebellar interneurones, intracellular application of 20 μM microcystin, a protein phosphatase 1/2A inhibitor, prolonged (63 ± 14%; mean ± S.E.M.) the decay time course of miniature IPSCs (mIPSCs) without significantly affecting their amplitude, rise time and frequency. The effect of microcystin could be blocked by co-applying PKA inhibitory peptide (PKA-I, 1 μM).

4. No significant changes in any of the mIPSC parameters could be detected after intracellular application of PKA-I alone or following the inhibition of calcineurin with FK506 (50 nM).

5. In granule cells of the olfactory bulb expressing the $\beta3$ subunit fast and slowly rising mIPSCs were detected, resulting in a bimodal distribution of the 10–90% rise times, suggesting two distinct populations of events. Fast rising mIPSCs ($mIPSC_{FR}$) had a 10–90% rise time of 410 ± 50 μs, an amplitude of 68 ± 6 pA, and a weighted decay time constant (τ_w) of $15{\cdot}8 \pm 2{\cdot}9$ ms. In contrast, slowly rising mIPSCs ($mIPSC_{SR}$) displayed an approximately threefold slower rise time ($1{\cdot}15 \pm 0{\cdot}12$ ms), 57% smaller amplitude ($29 \pm 1{\cdot}7$ pA), but had a τ_w ($16{\cdot}8 \pm 3{\cdot}0$ ms) similar to that of the fast events.

6. mIPSCs in olfactory granule cells were not affected by the intracellular perfusion of microcystin. In spite of this, intracellular administration of constitutively active PKA caused a small, gradual, but significant increase (18 ± 5%) in the amplitude of the events without changing their time course.

7. These findings demonstrate a cell-type-dependent regulation of synaptic inhibition by protein phosphorylation. Furthermore, our results show that the effect of PKA-mediated phosphorylation on synaptic inhibition depends upon the subunit composition of postsynaptic $GABA_A$ receptors.

Diverse functional requirements of the CNS are fulfilled by the activation of $GABA_A$ receptors, and this may be accomplished through their molecular specialisation (Sieghart, 1995), specific subcellular placement (Nusser *et al.* 1996) and selective regulation (McDonald *et al.* 1998) as well as through highly specialised GABA-releasing neurones (Freund & Buzsaki, 1996). There is a wealth of information on how molecular diversity influences the kinetics and pharmacological properties of $GABA_A$ receptor channels (reviewed by Macdonald & Olsen, 1994; Sieghart, 1995), but much less is known about the regulation of synaptic $GABA_A$ receptor function by protein kinases (Jones & Westbrook, 1997; Poisbeau *et al.* 1999). In human embryonic kidney (HEK 293) cells expressing recombinant $GABA_A$ receptors, phosphorylation by cAMP-dependent protein kinase (PKA) of receptors containing the $\beta1$-type β subunit has been

shown to decrease whole-cell responses to GABA (Moss *et al.* 1992; McDonald *et al.* 1998), whereas phosphorylation of receptors containing the β3-type β subunit enhanced GABA-evoked currents. Meanwhile, β2 subunit-containing receptors were not affected by PKA (McDonald *et al.* 1998). These results demonstrate the critical role played by the β subunits in determining the functional consequences of PKA phosphorylation. The great advantage of using recombinant receptors in expression systems (Kellenberger *et al.* 1992; Moss *et al.* 1992; Leidenheimer, 1996; McDonald *et al.* 1998) is the known subunit composition of the receptors and the possibility to examine any given subunit combination. However, these receptors are not concentrated at synaptic junctions, where they are in a special 'microenvironment' with a fine balance of associated proteins, cytoskeletal elements and regulatory enzymes (Essricht *et al.* 1998; Hanley *et al.* 1999; Wang *et al.* 1999).

Furthermore, functional experiments in expression systems are regularly performed under 'equilibrium conditions', which are unlike those present during synaptic transmission. Responses to low concentrations of GABA (10 μM) applied for several seconds may be affected differentially to those evoked by a relatively high concentration of GABA (0·3–3 mM) believed to be present only for a very short period (< 1 ms) in the synaptic cleft (Clements, 1996; Jones & Westbrook, 1996; Mozrzymas *et al.* 1999; Perrais & Ropert, 1999). These conditions can be mimicked by using ultrafast agonist applications to outside-out patches excised from cells expressing $GABA_A$ receptors (Puia *et al.* 1994; Jones & Westbrook, 1996, 1997; Lavoie & Twyman, 1996). However, phosphorylation experiments require an intact intracellular milieu, with all the enzymatic machinery and energy sources, as well as intact protein–protein interactions linking together the receptors, cytoskeletal elements and regulatory enzymes (Moss & Smart, 1996). All of these may not be preserved during patch excision, limiting the use of excised patches for studying the role of protein phosphorylation in receptor function. Probably the best way to study the role of protein phosphorylation in $GABA_A$ receptor function is to investigate its effects on inhibitory postsynaptic currents (IPSCs) using either neuronal cultures or acute brain slices (Jones & Westbrook, 1997; Poisbeau *et al.* 1999). Unfortunately, this approach has some limitations too. Most nerve cells express a large number of $GABA_A$ receptor subunits (Persohn *et al.* 1992; Wisden *et al.* 1992; Fritschy & Mohler, 1995; Sperk *et al.* 1997) that co-assemble into several distinct $GABA_A$ receptor subtypes with largely unknown subunit composition. Thus, in most neurones inhibitory synaptic currents result from the activation of diverse populations of receptor subtypes. For example, the effect of protein phosphorylation on synaptic $GABA_A$ receptor function has been studied in hippocampal pyramidal cells (Poisbeau *et al.* 1999), which express at least nine distinct subunits, generating an unknown number of receptor subtypes with diverse subunit assemblies. Thus, a subtype-specific regulation of synaptic $GABA_A$ receptor function by protein phosphorylation cannot be easily revealed in such cells. To overcome this limitation, we have chosen an approach to compare the effects of protein phosphorylation on synaptic $GABA_A$ receptor function in nerve cells, which express only a limited number of $GABA_A$ receptor subtypes. Special care was taken to choose nerve cells expressing only a single type of β subunit, as β subunits have a critical role in PKA-dependent phosphorylation (McDonald *et al.* 1998). We found that granule cells of the olfactory bulb express only β3 as the β subunit variant, whereas cerebellar stellate and basket cells contain β2 as the only β subunit. According to our results, phosphorylation by PKA differentially affects synaptic $GABA_A$ receptor function in these cells. The amplitude of mIPSCs in olfactory granule cells was increased by PKA phosphorylation without affecting mIPSC kinetics, whereas only the decay time course of mIPSCs was prolonged in cerebellar interneurones.

METHODS

Slice preparation and electrophysiological recordings

Seventeen- to 30-day-old (P17–P30, 20·3 ± 0·8 days (mean ± S.E.M.), $n = 19$ mice; for cerebellar stellate cells: P17–P30, 20·7 ± 1·2 days, $n = 10$ mice, total of 23 cells; for olfactory granule cells: P17–P25, 19·9 ± 0·9 days, $n = 9$ mice, total of 16 cells) C57Black6 mice were anaesthetised with halothane before decapitation, in accordance with the guidelines of the UCLA Office for Protection of Research Subjects. The brains were then removed and placed into an ice-cold artificial cerebrospinal fluid (ACSF) containing (mM): 126 NaCl, 2·5 KCl, 2 $CaCl_2$, 2 $MgCl_2$, 1·25 NaH_2PO_4, 26 $NaHCO_3$ and 10 D-glucose, pH 7·3 when bubbled with 95% O_2 and 5% CO_2. The cerebellum or the olfactory bulb was glued to a platform, and 300 μm-thick sagittal slices were cut with a Vibratome (Lancer Series 1000). The slices were stored submerged at 32 °C in ACSF until they were transferred to the recording chamber.

During recording, the slices were continuously perfused with 32 °C ACSF containing 3–5 mM kynurenic acid and 1 μM tetrodotoxin. All recordings were made from the somata of visually identified neurones (Zeiss Axioscope infrared differential interference contrast (IR-DIC) videomicroscopy, ×40 water immersion objective) with an Axopatch 200B amplifier (Axon Instruments). Patch electrodes were pulled (Narishige PP-38, Tokyo) from thick-walled borosilicate glass (o.d. = 1·5 mm, i.d. = 0·86 mm; Sutter Instruments) and were filled with a solution containing (mM): 140 CsCl, 4 NaCl, 1 $MgCl_2$, 10 Hepes, 0·05 EGTA, 2 MgATP and 0·4 MgGTP. All solutions were titrated to a pH of 7·25 and an osmolarity of 280–290 mosmol l^{-1}. The resistance of the electrodes was between 5 and 8 MΩ when filled with pipette solution. Special care was taken that after establishing the whole-cell configuration, the series resistance was quickly compensated and recordings were started within tens of seconds. Series resistance and whole-cell capacitance were estimated by compensating the fast current transients evoked at the onset and offset of 8 ms-long 5 mV voltage-command steps and were checked every 2 min during the recording. If the access resistance increased by more than 50%, the recording was discontinued. The access resistance remaining after 75–80% compensation (with 7–8 μs lag values) was 3·1 ± 0·2 MΩ for cerebellar interneurones and 3·1 ± 0·3 MΩ for olfactory granule cells.

Data analysis

All recordings were low-pass filtered at 2 kHz (8-pole Bessel, Frequency Devices 902) and digitised on-line at 20 kHz using a PCI-MIO 16E-4 data acquisition board (National Instuments, Austin, TX, USA) and WinCDR1.3 software (courtesy of Dr J. Dempster, University of Strathclyde, Glasgow, UK) running on a Pentium II IBM/AT compatible computer. Miniature currents were detected in WinCDR1.3 and the events after detection and subtraction were analysed using WCP2.1 software (courtesy of Dr J. Dempster). The amplitudes, 10–90% rise times, 50% decay times and inter-event intervals of mIPSCs were measured and the decay of the averaged currents was fitted with a single exponential or the sum of two exponential functions. The weighted decay time constant (τ_w) was calculated as $\tau_w = \tau_1 A_1 + \tau_2(1 - A_1)$, where τ_1 and τ_2 are the time constants of the first and second exponential functions, respectively, and A_1 is the proportion of the first exponential function contributing to the amplitude of the IPSC. Data are expressed as means ± S.E.M.

Solutions and drugs

Kynurenic acid and tetrodotoxin were purchased from Sigma and Calbiochem (La Jolla, CA, USA), respectively. Microcystin-LR (Calbiochem) was first prepared as a 20 mM stock solution in DMSO, and this was diluted 1000 times in the intracellular solution, resulting in a final concentration of 20 μM microcystin-LR and 0·1% DMSO. Constitutively active catalytic subunit of PKA was prepared from bovine heart as described previously (Browning *et al.* 1990) and was a generous gift of Dr M. D. Browning, University of Colorado, Denver, USA. The stock solution contained 300 μg ml^{-1} constitutively active catalytic subunit of PKA in a buffer containing 0·1 M NaCl, 10 mM Mes (pH 6·5), 30 mM β-mercaptoethanol, 0·1 mM EDTA and 50% ethylene glycol. A final concentration of 3 μg ml^{-1} was prepared by diluting the stock solution 100 times in the intracellular solution. PKA inhibitory peptide (PKA-I; H_2N-TYADFIASGRTGRRNAI-amide; final concentration, 1 μM) was a generous gift of Dr J. Haycock through Dr Browning, and was prepared from a stock solution containing 333 μM PKA-I in 0·1 M NaCl, 10 mM Mes (pH 6·5), 30 mM β-mercaptoethanol, 0·1 mM EDTA and 50% ethylene glycol. As shown by a previous study in our lab (Poisbeau *et al.* 1999), the vehicle in the presence of the deactivated peptide has no effect on neuronal function.

Immunohistochemistry

Light microscopic immunostaining for $GABA_A$ receptor subunits was performed as described previously (Somogyi *et al.* 1989; Nusser *et al.* 1995). C57Black6 mice (P20) were anaesthetised with halothane and were perfused through the heart with 0·9% saline for 1 min followed by a fixative containing 4% paraformaldehyde, 0·05% glutaraldehyde and ~0·2% picric acid made up in 0·1 M phosphate buffer (PB, pH 7·4) for 20 min. The brains were then removed, and blocks from the cerebellum and olfactory bulb were cut out and washed in PB. Vibratome sections (70 μm thick) were cut and were collected in PB. Normal goat serum (20%) was used in 50 mM Tris-HCl (pH 7·4) containing 0·9% NaCl (TBS) as the blocking solution for 0·5 h followed by incubation overnight with purified primary antibody diluted in TBS containing 1% normal goat serum and 0·05% Triton X-100. The primary antibodies were used at the following final concentrations: β1 (code no. β1(350-404)R16/6, Jechlinger *et al.* 1998), 1·25 μg ml^{-1}; β2 (code no. β2(351-405)R20, Jechlinger *et al.* 1998), 1·9 μg ml^{-1}; and β3 (code no. β3(345-408)R21, Slany *et al.* 1995), 1 μg ml^{-1}. The sections were washed, then incubated for 90 min in biotinylated secondary antibody (goat anti-rabbit, diluted 1:50 in TBS; Vector Laboratories, Burlingame, CA, USA), followed by further washing and incubation in avidin-biotinylated horseradish peroxidase complex (1:100 dilution in TBS) for 2 h. The peroxidase enzyme reaction was carried out with 3,3′-diaminobenzidine tetrahydrochloride as the chromogen and H_2O_2 as the oxidant. The sections were then routinely processed for light microscopic examination (Somogyi *et al.* 1989). No specific labelling was observed when the primary antibodies were either omitted or replaced by normal goat serum.

RESULTS

Differential expression of $GABA_A$ receptor β subunits in cerebellar interneurones and in olfactory granule cells

In situ hybridisation studies (Persohn *et al.* 1992; Wisden *et al.* 1992) indicated that several cell types, including interneurones in the molecular layer of the cerebellum, neurones in the globus pallidus and relay neurones in some nuclei of the thalamus, express mRNA for only the β2-type β subunit. As GABAergic synaptic currents can be recorded from cerebellar interneurones with a very high signal-to-noise ratio (Llano & Gerschenfeld, 1993; Auger & Marty, 1997; Nusser *et al.* 1997), we decided to examine the expression of every β subunit in the mouse cerebellar cortex using subunit-specific antibodies and light microscopic immunocytochemistry. Immunoreactivity for the β1 subunit was present in some astrocytes in the granule cell layer and in cell bodies and processes of Bergmann glia in the Purkinje cell and molecular layers (Fig. 1*A*). No detectable level of reactivity was observed in any neuronal cells. The β2 subunit had a widespread distribution in the cerebellar cortex (Nusser *et al.* 1999). The granule cell layer was strongly immunopositive for this subunit. In the molecular layer, immunostaining of the neuropile originated from Purkinje cell dendrites and from the basket and stellate cells. The cell bodies of interneurones were strongly outlined by the reaction end product (Fig. 1*B*, arrows). Immunoreactivity for the β3 subunit was restricted to the granule cell layer, where strongly immunopositive glomeruli appeared as dark rings with a pale centre, representing the immunonegative mossy fibre terminals in the middle and the stained granule cell dendrites at the periphery of the glomeruli (Fig. 1*C*). These results, in good agreement with *in situ* hybridisation studies, demonstrate that stellate and basket cells in the cerebellar molecular layer express only the β2-type β subunit protein at a detectable level. Furthermore, these cells also express the α1 and γ2 subunits (Persohn *et al.* 1992; Nusser *et al.* 1999), very probably forming a single $GABA_A$ receptor subtype with α1β2γ2 subunit composition (Jechlinger *et al.* 1998).

Although several cell types express mRNA for the β3 subunit in the CNS, in most cells the mRNA for this subunit is present together with the mRNA for other β subunits, with the possible exception of the granule cells in the main olfactory bulb (Persohn *et al.* 1992; Wisden *et al.* 1992). To test the distribution of all β subunits in the main olfactory bulb, we applied light microscopic immunohistochemistry

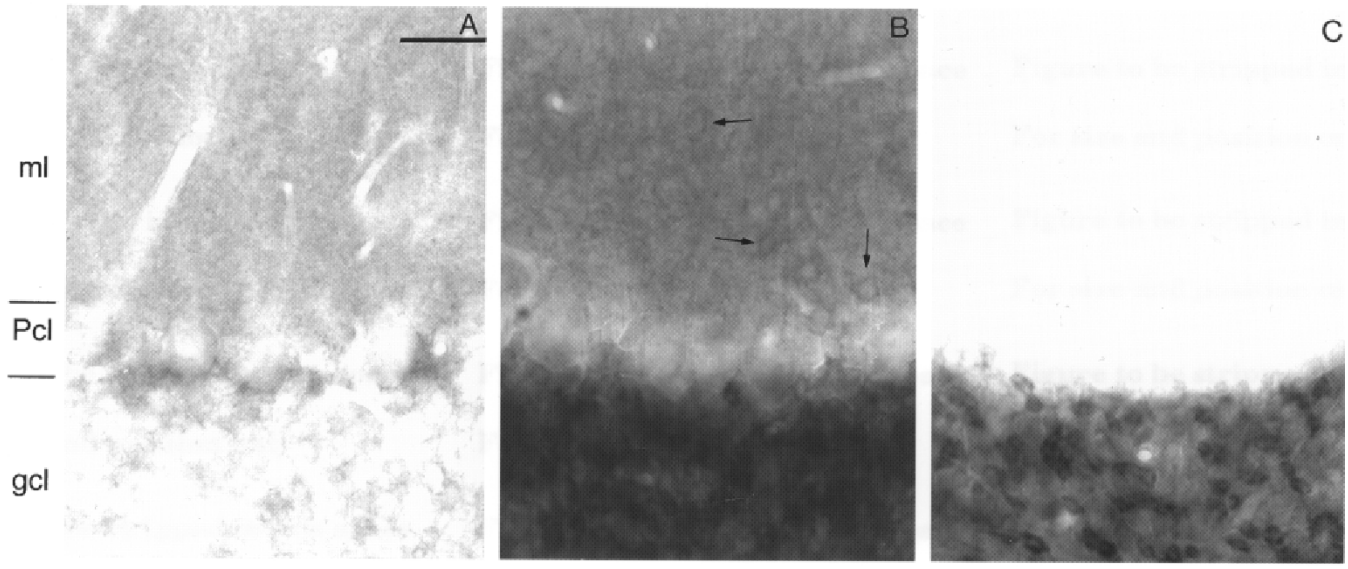

Figure 1. Distribution of immunoreactive β1, β2 and β3 subunits of the $GABA_A$ receptor in the cerebellar cortex of a P20 mouse using subunit-specific antibodies

A, Bergmann glia processes in the Purkinje cell layer (Pcl) and in the molecular layer (ml) showing immunoreactivity for the β1 subunit. Some astrocytes were also labelled in the granule cell layer (gcl). *B*, the β2 subunit was expressed by granule cells, Purkinje cells and interneurones of the molecular layer (arrows). *C*, the β3 subunit was exclusively present in the granule cell layer, where glomeruli appear as dark rings dominating the weakly reactive granule cell bodies. *A–C*, same magnification. Scale bar, 25 μm.

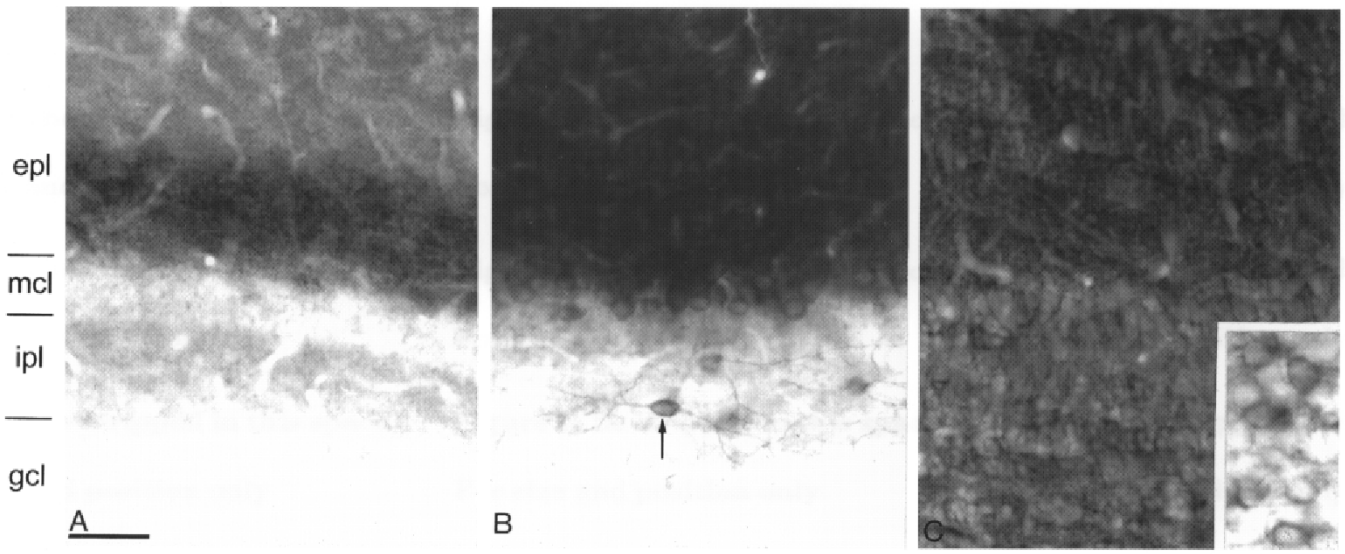

Figure 2. Light microscopic demonstration of immunoreactivity for the β1, β2 and β3 subunits in the main olfactory bulb of a P20 mouse using subunit-specific antibodies

A, strong immunostaining for the β1 subunit was detected in the inner one-third of the external plexiform layer (epl), the rest of the external plexiform layer being moderately labelled. No immunostaining was detected in the granule cell layer (gcl). *B*, mitral cells were strongly labelled for the β2 subunit, resulting in the intense staining of the mitral cell layer (mcl) and the external plexiform layer. In the internal plexiform layer (ipl) and granule cell layer, only short axon cells (e.g. arrow) were stained for this subunit. *C*, the β3 subunit was strongly expressed in all layers of the olfactory bulb. Granule cells were outlined by the reaction end product (see inset). *A–C*, same magnification. Scale bar: *A–C*, 50 μm; inset, 20 μm.

with subunit-specific antibodies in this brain region. The granule cell layer of the main olfactory bulb showed strong labelling for the β3 subunit, without any detectable staining for the β1 and β2 subunits (Fig. 2). At high magnification, it was apparent that the immunostaining of the granule cell layer originated from granule cells as every granule cell body was surrounded by the reaction end product (Fig. 2*C*). The external plexiform layer was strongly labelled for all β subunits (Fig. 2), demonstrating that mitral and tufted cells express a large variety of GABA$_A$ receptor subtypes, as found in cortical and hippocampal pyramidal cells. Granule cells, in addition to expressing β3 as the only β subunit, also strongly express the α2, α5, γ2 and δ subunits (Fritschy & Mohler, 1995), forming at least two main receptor subtypes (McKernan & Whiting, 1996; Barnard *et al.* 1998).

Unfortunately, we were unable to identify a single type of nerve cell expressing β1 as the sole β subunit. This is in agreement with *in situ* hybridisation data (Persohn *et al.* 1992; Wisden *et al.* 1992). Interestingly, Bergmann glial cells of the cerebellar cortex do express β1 as the only β subunit (Fig. 1), but unfortunately, glial cells are not amenable for the study of synaptic GABA$_A$ receptor function. Given this differential distribution of β subunits in cerebellar interneurones and olfactory granule cells, the regulation of synaptic GABA$_A$ receptor function was studied in these two cell types.

Regulation of synaptic GABA$_A$ receptor function by PKA phosphorylation in cerebellar stellate and basket cells

Miniature, GABA$_A$ receptor-mediated IPSCs were recorded from the somata of cerebellar interneurones of P17–P30 mice with CsCl-containing electrodes ($E_{Cl} \approx 0$ mV) at a holding potential of -60 mV in the presence of 3–5 mM kynurenic acid and 1 μM TTX (Fig. 3). Synaptic currents occurred with a frequency of $3{\cdot}8 \pm 1{\cdot}0$ Hz ($n = 6$ cells), had fast rise times (10–90% rise time, 280 ± 30 μs), variable amplitudes (range, 10–560 pA; Fig. 4) and decay time courses best described by the sum of two exponentials. The fast component had a time constant of $2{\cdot}0 \pm 0{\cdot}2$ ms and contributed to 52 ± 5% of the amplitude. The slow component had a time constant of $6{\cdot}6 \pm 1$ ms, resulting in a weighted time constant (τ_w) of $4{\cdot}2 \pm 0{\cdot}7$ ms. During the course of 9 min whole-cell recordings in the control condition, there was no significant ($P > 0{\cdot}15$, paired t test, $n = 6$) change in the frequency (1st minute, $3{\cdot}8 \pm 1{\cdot}0$ Hz; 9th minute, $4{\cdot}5 \pm 1{\cdot}4$ Hz), 10–90% rise time (1st minute, 280 ± 30 μs; 9th minute, 300 ± 20 μs), or amplitude (1st minute, 112 ± 10 pA; 9th minute, 108 ± 15 pA) of the events (Fig. 5). The weighted decay times of mIPSCs were $4{\cdot}2 \pm 0{\cdot}7$ ms during the first minute and $5{\cdot}1 \pm 0{\cdot}5$ ms during the ninth minute of recording, but these values were not significantly different from each other ($P = 0{\cdot}07$, paired t test).

To test whether endogenous phosphatase/kinase activities play a role in the regulation of synaptic GABA$_A$ receptor function in cerebellar interneurones, 20 μM microcystin, a cell-impermeant protein phosphatase 1/2A (PP1/2A) inhibitor, was applied intracellularly and its effect on the synaptic currents was examined. Nine minutes after establishing the whole-cell configuration, the frequency (9th minute = 88 ± 8% of 1st minute, $n = 5$), rise time (103 ± 3%) and amplitude (103 ± 16%) of the events did not change significantly ($P > 0{\cdot}18$, paired t test; Fig. 4), but the decay time course was prolonged to 163 ± 14% of that measured in the first minute of the recordings (1st minute, $\tau_w = 5{\cdot}1 \pm 0{\cdot}4$ ms; 9th minute, $\tau_w = 8{\cdot}1 \pm 0{\cdot}4$ ms; $n = 5$, $P < 0{\cdot}01$, paired t test; Figs 3–5). This prolongation of the time course was due to a 48 and 52% increase in τ_1 and τ_2,

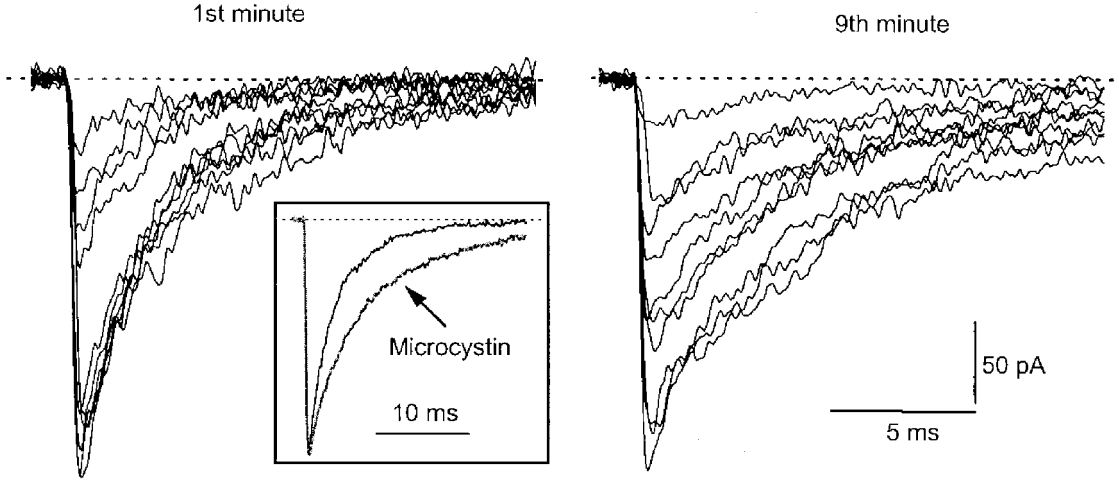

Figure 3. Effect of intracellularly applied microcystin on mIPSCs recorded from an interneurone in the cerebellar molecular layer

Ten consecutive mIPSCs recorded in the first (left panel) and ninth minute (right panel) after establishing the whole-cell configuration. The amplitude of the synaptic currents and its variability were not altered, but the decay time course was prolonged by 20 μM microcystin. The average current waveforms in the first and ninth minutes are shown in the inset. CsCl-based intracellular solution was used and the cell was held at -60 mV.

respectively, without a significant change in their relative contributions to the amplitude ($A_1 = 58\%$ at 1st minute *vs.* $A_1 = 55\%$ at 9th minute). Thus, there must be a continuously active kinase phosphorylating the receptors or some related proteins, as blocking the activity of PP1/2A resulted in a change in the decay of mIPSCs. Furthermore, we could not find evidence for the involvement of calcineurin (PP2B) in the regulation of synaptic $GABA_A$ receptor function in cerebellar interneurones, as the application of 50 nM FK506 did not significantly ($P > 0{\cdot}14$, paired t test) change any of the measured parameters (amplitude, $103 \pm 2\%$; rise time, $96 \pm 4\%$; τ_w, $111 \pm 14\%$; frequency, $114 \pm 22\%$; $n = 3$). These results demonstrate that continuous phosphorylation–dephosphorylation processes are involved in the regulation of mIPSCs in cerebellar interneurones, PP1/2A being responsible for the continuous dephosphorylation of either the $GABA_A$ receptors or some other associated proteins.

To identify the kinase involved in the phosphorylation, we included a specific inhibitory peptide of PKA (PKA-I, 1 μM; see Methods) in the patch pipette solution together with 20 μM microcystin to suppress the activity of both PP1/2A and the endogenous PKA. The inclusion of PKA-I had no significant effect on the frequency, amplitude or rise time of the events, but counteracted the effect of microcystin on the decay of the synaptic currents (9th minute $= 115 \pm 9\%$ of 1st minute, $n = 4$ cells; Fig. 6), demonstrating that PKA activity is responsible for the phosphorylation when phosphatases are inhibited. Thus, it is very likely that there is a continuous cycle of phosphorylation by PKA and dephosphorylation by PP1/2A of synaptic $GABA_A$ receptors in cerebellar interneurones. Furthermore, $GABA_A$ receptors or some associated proteins are not fully phosphorylated under control conditions, as blocking PP1/2A enhanced their phosphorylation state. If these proteins were not fully dephosphorylated, blocking the

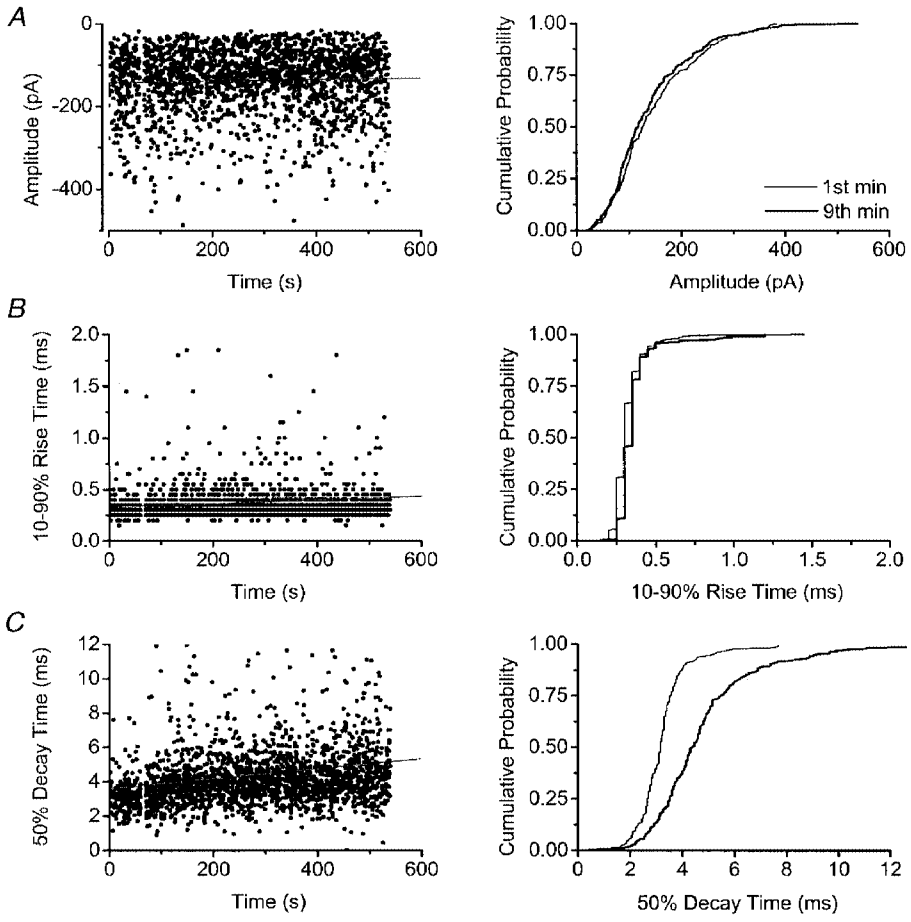

Figure 4. Microcystin prolongs the decay time of mIPSCs recorded in a cerebellar interneurone
A, during the 9 min of whole-cell recordings, there was no significant change in the amplitude of mIPSCs (slope of regression line, 0·017; $r = 0{\cdot}03$), which can also be seen on the cumulative probability plot (right panel), comparing the distribution of mIPSC amplitudes in the first (thin line) and ninth (thick line) minute. *B*, similarly to the results for amplitude, 20 μM microcystin had no effect on the 10–90% rise time of mIPSCs throughout the recordings (slope of regression line, $1{\cdot}7 \times 10^{-4}$; $r = 0{\cdot}05$). The right panel shows the cumulative distribution of mIPSC rise times in the first and ninth minute of whole-cell recording. *C*, the 50% decay time of mIPSCs was prolonged by microcystin as the slope of the regression line was significantly (slope, 0·03; $r = 0{\cdot}17$; $P < 0{\cdot}0001$, t test) different from zero. Furthermore, the cumulative distribution of the 50% decay times (right panel) in the ninth minute was also significantly different ($P < 0{\cdot}001$, Kolmogorov–Smirnov test) from that during the first minute.

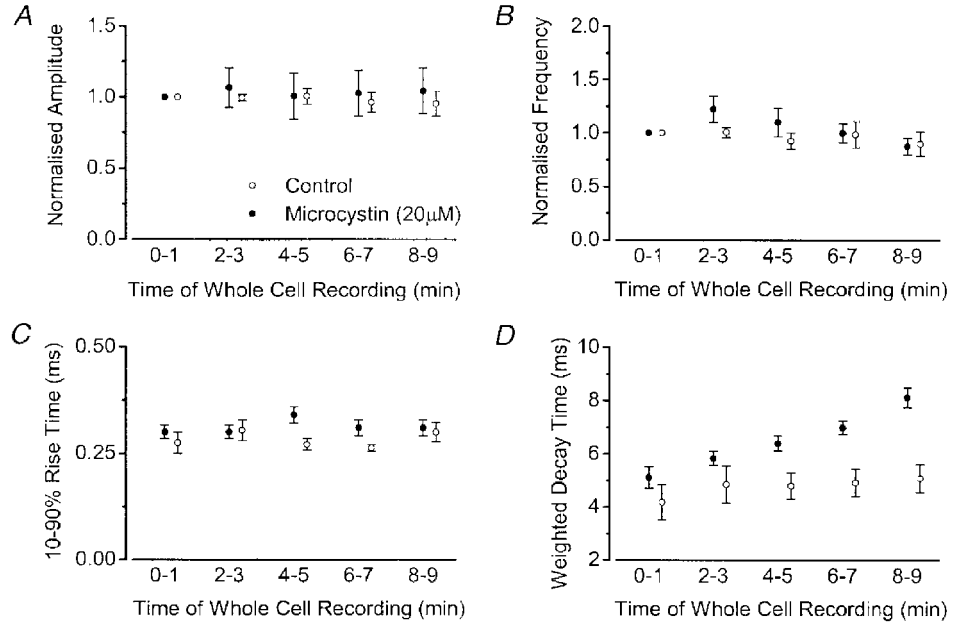

Figure 5. Summary of the effect of 20 μM microcystin on the amplitude, frequency and kinetics of mIPSCs recorded in cerebellar interneurones

mIPSCs were collected during the first minute and during every consecutive 2 min and the mean ± S.E.M. of their normalised peak amplitudes (*A*), normalised frequencies (*B*), 10–90% rise times (*C*) and weighted decay times (*D*) were calculated and plotted (○, control, $n = 6$; ●, microcystin, $n = 5$). There were no significant changes in the amplitudes, frequencies and rise times of the events in control and in microcystin within the 9 min of recording. In contrast, the decay time course of the events was significantly prolonged by microcystin from the fourth minute onwards. In cells where longer recordings were made no significant prolongation in the decay occurred after the ninth minute.

activity of the kinase without blocking that of the phosphatase should result in an acceleration of the decay of the synaptic currents. To test this possibility, we included 1 μM PKA-I without microcystin in the intracellular solution and tested its effect on the synaptic currents. PKA-I on its own did not accelerate the rate of decay of the synaptic currents (1st minute, $\tau_w = 4{\cdot}4 \pm 0{\cdot}3$ ms; 7th minute, $\tau_w = 4{\cdot}8 \pm 0{\cdot}3$ ms; $n = 3$), suggesting that the phosphorylation state of the proteins involved is overwhelmingly controlled by a strong phosphatase activity. Under control conditions, the rate of dephosphorylation of these proteins is probably faster than the rate of phosphorylation. However, after establishing the whole-cell configuration, our intracellular solution may shift the phosphorylation–dephosphorylation balance towards a more phosphorylated state, producing a slight slowing down of the decay.

Characterisation of $GABA_A$ receptor-mediated mIPSCs in granule cells of the main olfactory bulb

Whole-cell recordings were made from the somata of visually identified granule cells in acute olfactory bulb slices of P17–P25 mice with CsCl-containing pipettes. As there have been no previous studies of mIPSCs in this cell type, we began by characterising the basic properties of the synaptic currents. In the presence of the sodium channel

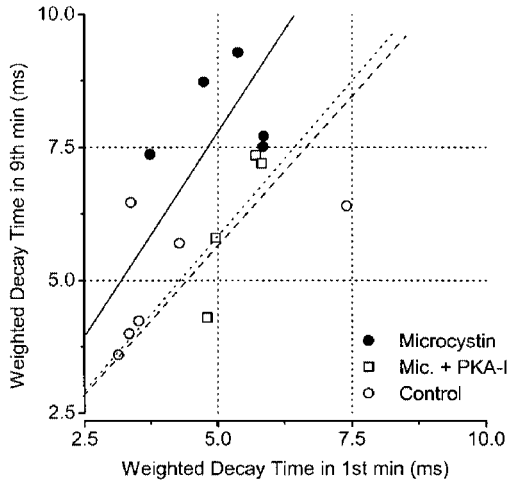

Figure 6. Intracellular application of PKA-I prevents the prolongation of mIPSC decay by microcystin in cerebellar interneurones

The weighted decay time of mIPSCs in the first minute is plotted as a function of that measured in the ninth minute of whole-cell recording in 20 μM microcystin (●, $n = 5$ cells), microcystin + 1 μM PKA-I (□, $n = 4$) and control (○, $n = 6$). The slopes of the regression lines forced to intersect the origin were 1·55 in microcystin (continuous line), 1·17 in microcystin + PKA-I (dotted line) and 1·13 in control (dashed line). Thus, the application of PKA-I counteracted the effect of microcystin on the decay time course.

blocker TTX (1 μM) and an ionotropic glutamate receptor blocker, kynurenic acid (3–5 mM), spontaneously occurring inward currents were observed. These currents were blocked by the selective $GABA_A$ receptor antagonist bicuculline methiodide (20 μM). The synaptic currents had variable amplitudes, resulting in a skewed amplitude distribution (Fig. 7), similar to that found in several other cell types. mIPSCs occurred with a mean frequency of $0{\cdot}7 \pm 0{\cdot}25$ Hz

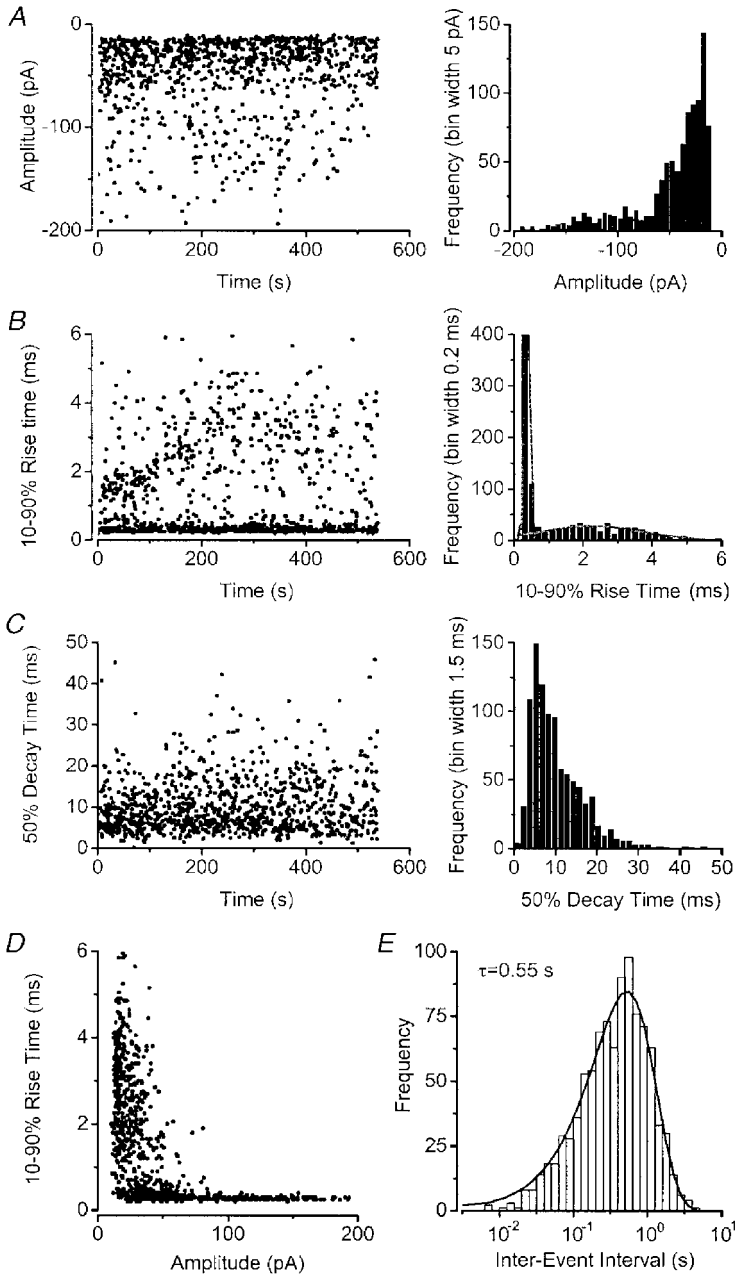

Figure 7. Characterisation of mIPSCs recorded in an olfactory granule cell

A, the amplitudes of mIPSCs showed a large variability, but remained constant throughout the 9 min of this whole-cell recording. The amplitude distribution of mIPSCs was skewed towards larger values with a mean of −48·8 pA and coefficient of variation (c.v.) of 0·8. *B*, there was a large variability in the 10–90% rise times of the synaptic events (c.v. = 1·02). Most events had rise times of less than 500 μs, but other events had rise times of up to 6 ms. The bimodal distribution of the 10–90% rise times could be well described by the sum of two Gaussian distributions (first, $0{\cdot}37 \pm 0{\cdot}06$ ms; second, $2{\cdot}2 \pm 1{\cdot}5$ ms; means ± S.D.), consistent with the existence of at least two populations of mIPSCs in olfactory granule cells. *C*, the 50% decay times of the synaptic currents remained constant during the recording in control conditions. The distribution of 50% decay times was skewed with a mean of 10·3 ms and a c.v. of 0·68. *D*, scatter plot of amplitude *vs.* 10–90% rise time showing that the slowly rising events on average had smaller amplitudes than those with fast rise times. *E*, log-binned inter-event intervals (10 bins decade^{-1}) were well fitted by a single exponential function ($\tau = 0{\cdot}55$ s), consistent with a random occurrence of mIPSCs. Data in *A*–*E* are from the same cell (P20 mouse).

($n = 6$). The distribution of inter-event intervals could be well fitted with a single exponential function (Fig. 7), consistent with a random occurrence of the mIPSCs. Interestingly, in most cells both fast and slowly rising mIPSCs were observed (Fig. 8), resulting in a bimodal distribution of the 10–90% rise times (Fig. 7), which suggests the presence of at least two populations of mIPSCs. Indeed, the sum of two Gaussians fitted the 10–90% rise time distribution significantly better than a single Gaussian (Fig. 7*B*; $P < 0{\cdot}01$, F test). While mIPSCs with slow rise times always had small amplitudes (10–50 pA), fast rising mIPSCs had variable amplitudes, ranging from tens to several hundreds of picoamps (Fig. 7). This correlation between the amplitude and the rise time of the events can easily be explained by dendritic filtering of some synaptic currents originating distally on the dendritic tree. When mIPSCs with less than 1 ms 10–90% rise times were averaged (fast rising mIPSCs, mIPSC$_{FR}$), they had approximately three times faster rise times ($0{\cdot}41 \pm 0{\cdot}05$ *vs.* $1{\cdot}15 \pm 0{\cdot}12$ ms, $n = 5$ cells) and peak amplitudes more than two times larger (68 ± 6 *vs.* 29 ± 2 pA) than the slowly rising mIPSCs (mIPSC$_{SR}$). However, fast and slowly rising mIPSCs had very similar weighted decay times ($15{\cdot}8 \pm 2{\cdot}9$ *vs.* $16{\cdot}8 \pm 3$ ms, respectively), which is inconsistent with dendritic filtering alone being responsible for the two populations of events. Figure 8 shows a representative cell,

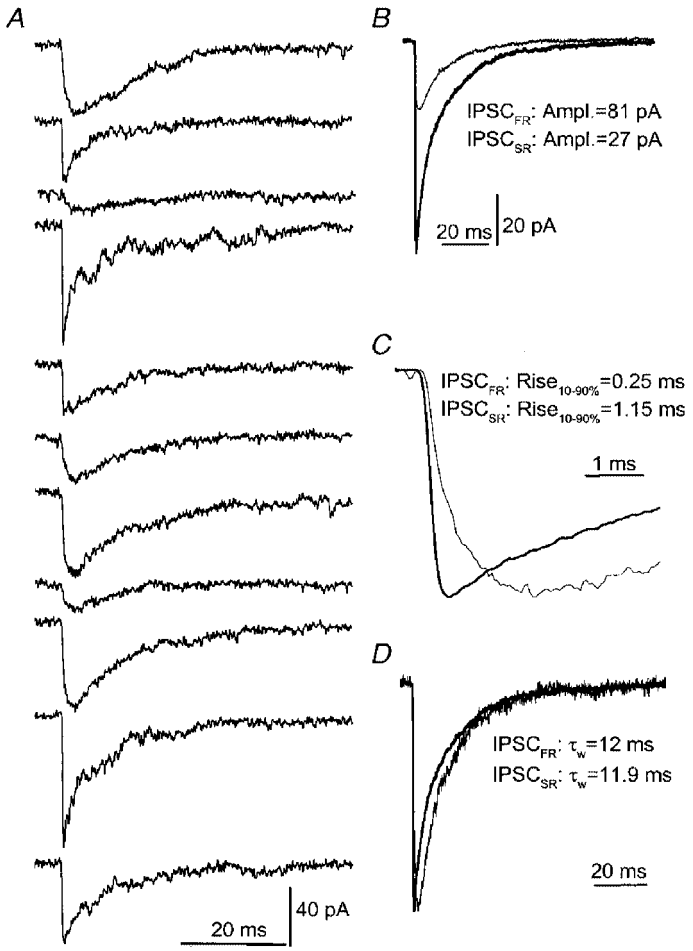

Figure 8. Fast and slowly rising mIPSCs recorded in a granule cell of the main olfactory bulb

A, 11 consecutive mIPSCs recorded from a P20 mouse olfactory granule cell (same cell as in Fig. 7) showing large variability in their amplitudes and rise times. The GABA$_A$ receptor-mediated mIPSCs were inward currents as the intracellular solution contained a high concentration of Cl^- ($E_{Cl} \approx 0$ mV) and the cell was held at −60 mV. *B*, mIPSCs with faster than 1 ms 10–90% rise times (mIPSC$_{FR}$, thick trace) were averaged and compared to the average of slowly rising mIPSCs (mIPSC$_{SR}$, thin trace; 10–90% rise times > 1 ms). mIPSC$_{SR}$ had an approximately three times smaller amplitude (27 *vs.* 81 pA) than mIPSC$_{FR}$. *C*, the 10–90% rise time of the averaged mIPSC$_{FR}$ was four times faster than that of the mIPSC$_{SR}$ in this cell. *D*, despite mIPSC$_{SR}$ having a smaller amplitude and slower rise time, the weighted decay time constant was comparable to that of mIPSC$_{FR}$ (mIPSC$_{SR}$, $\tau = 11{\cdot}9$ ms; mIPSC$_{FR}$, $\tau_w = 12$ ms). A remarkable difference between the decay kinetics of the fast and slowly rising currents is that the sum of two exponential functions ($\tau_1 = 3{\cdot}4$ ms (40%), $\tau_2 = 17{\cdot}7$ ms, $\tau_w = 12$ ms; $\chi^2 = 0{\cdot}39$) always described the decay kinetics of the mIPSC$_{FR}$ significantly better than a single exponential ($\tau = 13{\cdot}3$ ms, $\chi^2 = 3{\cdot}0$), whereas a single exponential adequately fitted the decay of the mIPSC$_{SR}$ ($\tau = 11{\cdot}9$ ms, $\chi^2 = 0{\cdot}32$ *vs.* $\tau_1 = 2{\cdot}6$ ms (16%), $\tau_2 = 12{\cdot}8$ ms, $\tau_w = 11{\cdot}2$ ms, $\chi^2 = 0{\cdot}28$).

where $mIPSC_{FR}$ had a three times larger peak amplitude and more than four times faster 10–90% rise time, but a weighted decay time constant almost identical to that of $mIPSC_{SR}$. The strongest evidence in support of $mIPSC_{FR}$ and $mIPSC_{SR}$ having different kinetics at their respective sites of origin consists of the large difference in the charge transferred by the two types of events. The slowly rising mIPSCs ($0{\cdot}52 \pm 0{\cdot}06$ pC) carried only 55% of the charge measured for the fast rising currents ($0{\cdot}95 \pm 0{\cdot}01$ pC), inconsistent with the conservation of charge for similar synaptic events originating at different electrotonic locations. It is also interesting to note that the sum of two exponential functions always described the decay of $mIPSC_{FR}$ better than a single exponential, whereas no significant improvement was obtained when the $mIPSC_{SR}$ decay was fitted with two exponentials.

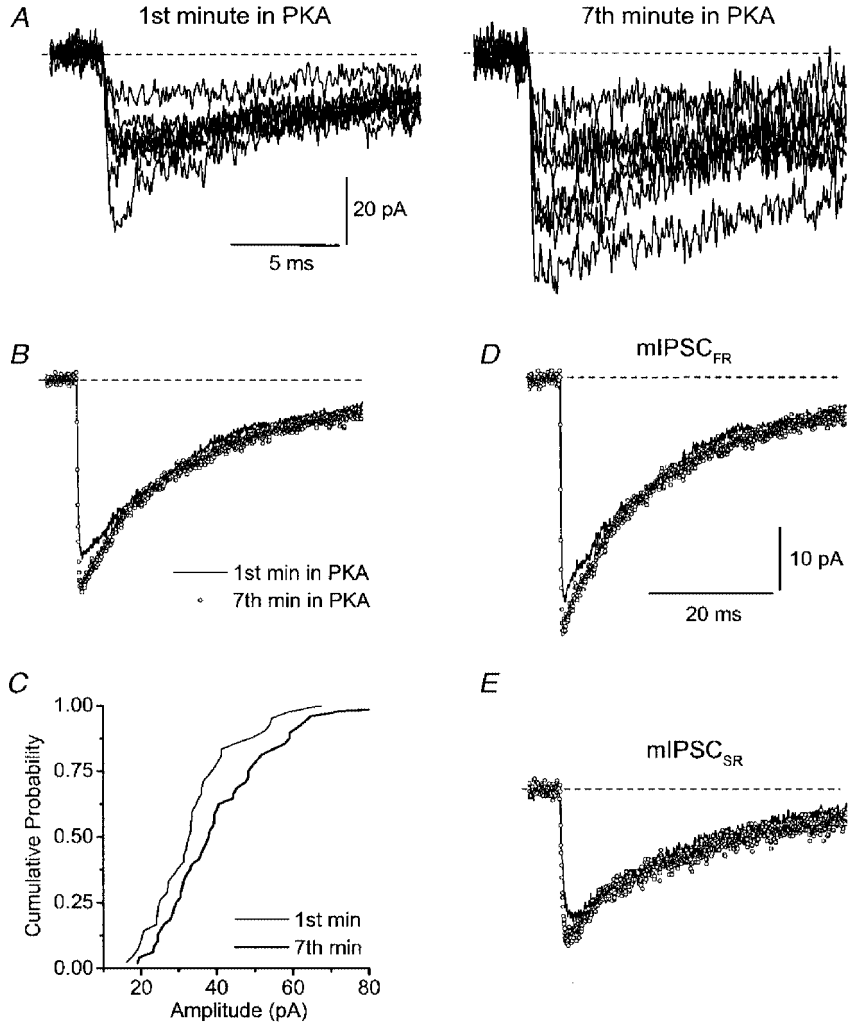

Figure 9. Constitutively active PKA increases the amplitude of mIPSCs recorded in a granule cell of the olfactory bulb

A, consecutive mIPSCs recorded during the first (left panel) and the seventh minute (right panel) after establishing the whole-cell configuration with intracellular solution containing 3 μg ml^{-1} constitutively active PKA. Note the increased amplitude of mIPSCs after 7 min of recording and the unaltered variability in the amplitudes. *B*, superimposed averaged synaptic currents recorded during the first (28·3 pA) and seventh minutes (33·5 pA) showing an 18% increase in the amplitude. The decay kinetics of the currents did not change significantly (1st minute, $\tau_w = 25{\cdot}2$ ms; 7th minute, $\tau_w = 23{\cdot}5$ ms). These means were obtained from every mIPSC regardless of their rise times. *C*, cumulative probability plot of the amplitudes of mIPSCs recorded in the first (thin line) and seventh minute (thick line) of whole-cell recording with intracellular solution containing 3 μg ml^{-1} constitutively active PKA, demonstrating a parallel shift in the distribution. The distributions contain every mIPSC in the first (mean = 34 pA, c.v. = 0·34, $n = 42$) and seventh minute (mean = 41 pA, c.v. = 0·38, $n = 48$). *D*, averaged mIPSCs with less than 1 ms 10–90% rise times in the first and seventh minutes of the recording showing an increase in the amplitude (18%, from 34·2 to 40·3 pA) similar to that of the pooled averages (*B*). No significant change was seen in the decay kinetics of the $mIPSC_{FR}$ (1st minute, $\tau_w = 23{\cdot}5$ ms; 7th minute, $\tau_w = 23{\cdot}0$ ms). *E*, the amplitude of the averaged $mIPSC_{SR}$ increased by 23%, from 20 to 24·7 pA, during the 7 min of recording without any significant alteration in the decay kinetics (1st minute, $\tau = 24{\cdot}5$ ms; 7th minute, $\tau = 26{\cdot}7$ ms).

Different kinetics of mIPSCs in the two cell types

In summary, we recorded $GABA_A$ receptor-mediated mIPSCs from granule cells of the main olfactory bulb in acute slices, which were heterogeneous with regard to their kinetic properties. Slow and fast rising mIPSCs could be distinguished, very probably owing to different kinetics at their sites of origin. The existence of two populations of mIPSCs is consistent with the presence of multiple $GABA_A$ receptor subtypes in olfactory granule cells. The different $GABA_A$ receptor subtypes demonstrated by immunocytochemistry ($\alpha2$, $\alpha5$, $\beta3$, $\gamma2$ and δ *vs.* $\alpha1$, $\beta2$ and $\gamma2$ subunits, respectively) in olfactory granule cells and cerebellar interneurones may be responsible for the synaptic currents with very different kinetics. The 10–90 % rise time of the granule cell $mIPSC_{FR}$ (410 ± 50 μs) is very similar to that recorded in cerebellar interneurones (280 ± 30 μs), suggesting a similar voltage control of the synapses generating these events in these two cell types. However, the weighted decay time of the $mIPSC_{FR}$ ($15{\cdot}8 \pm 2{\cdot}9$ ms) is almost four times slower than that of mIPSCs recorded in cerebellar interneurones ($4{\cdot}2 \pm 0{\cdot}7$ ms). A four times slower τ_1 ($8{\cdot}1 \pm 1{\cdot}6$ *vs.* $2{\cdot}0 \pm 0{\cdot}2$ ms) contributes to a similar proportion of the amplitude (65 *vs.* 52 %) and the τ_2 is approximately five times slower ($34{\cdot}6 \pm 8{\cdot}9$ *vs.* $6{\cdot}6 \pm 1{\cdot}0$ ms). Thus, the different $GABA_A$ receptor subtypes seem to generate mIPSCs with distinct kinetic properties. We next addressed whether regulation of synaptic $GABA_A$ receptor function in olfactory granule cells is also different from that in cerebellar interneurones.

Effect of phosphorylation by PKA on mIPSCs recorded in olfactory granule cells

To investigate whether continuous phosphorylation–dephosphorylation processes also regulate mIPSCs of olfactory granule cells, 20 μM microcystin was applied intracellularly. In contrast to cerebellar interneurones, the intracellular application of microcystin resulted in no significant change in the frequency (91 ± 8 % of control, $n = 5$), amplitude (94 ± 8 %) or decay kinetics (105 ± 8 %) of mIPSCs (includes both fast and slowly rising currents). Although we have not found evidence for a continuous cycle of phosphorylation–dephosphorylation of $GABA_A$ receptors by PP1/2A, we wanted to know whether mIPSCs in olfactory granule cells could be modified by PKA-dependent phosphorylation. The inclusion of 3 μg ml^{-1} constitutively active PKA in the intracellular solution resulted in no significant change ($P > 0{\cdot}18$, paired t test) in the frequency (98 ± 18 % of control, $n = 7$), 10–90 % rise time (104 ± 4 %) and weighted decay time (106 ± 12 %) of mIPSCs, but increased the amplitude of the synaptic currents by 18 ± 5 % ($P = 0{\cdot}01$, paired t test). As changes in the amplitude of the synaptic currents could, in theory, originate from changes in the access and input resistance of the cells during the recordings, we examined these possibilities and found no change in the access or input resistance of the cells that could have explained the increase in the peak amplitude. Figure 9 shows a representative cell where an average 18 % increase in the amplitude was detected without any significant change in the kinetics. When fast and slowly rising mIPSCs were analysed separately, a similar increase in the amplitude was found for $mIPSC_{FR}$ (18 %) and $mIPSC_{SR}$ (23 %). It should be noted that the paucity of $mIPSC_{SR}$ in several cells precluded the analysis of the two populations separately in every cell. Nevertheless, in the cells with a sufficiently high frequency of both types of event, PKA caused a similar increase in the amplitude of $mIPSC_{FR}$ and $mIPSC_{SR}$ (e.g. Fig. 9).

DISCUSSION

We have demonstrated that cerebellar molecular layer interneurones and granule cells of the main olfactory bulb express only a single type of β subunit of the $GABA_A$ receptor. Olfactory granule cells contain only the $\beta3$-type of the three known mammalian β subunits, whereas cerebellar molecular layer interneurones express exclusively the $\beta2$-type β subunit. In cerebellar interneurones, where a continuous cycle of phosphorylation–dephosphorylation regulates synaptic $GABA_A$ receptor function, PKA is responsible for the phosphorylation and PP1/2A for the dephosphorylation. Our results also indicate that in these cells the phosphorylation state of the proteins involved is mainly controlled by a strong phosphatase activity. The regulation of synaptic $GABA_A$ receptor function in olfactory granule cells is in sharp contrast to that found in cerebellar interneurones. As the application of microcystin did not result in any significant alteration of mIPSCs, we conclude that a continuous phosphorylation–dephosphorylation cycle is not responsible for the regulation of synaptic $GABA_A$ receptor function in these cells. The PKA-dependent phosphorylation in both olfactory granule cells and cerebellar interneurones leads to an increased synaptic charge transfer, but through different mechanisms.

Distinct kinetic properties of mIPSCs in cells expressing different $GABA_A$ receptor subtypes

The reported decay time constants of mIPSCs vary tremendously in central neurones, ranging from ~4 to over 100 ms (Edwards *et al.* 1990; Otis & Mody, 1992; Llano & Gerschenfeld, 1993; Jones & Westbrook, 1995; Auger & Marty, 1997; Nusser *et al.* 1997; Brickley *et al.* 1999; Mozrzymas *et al.* 1999; Perrais & Ropert, 1999). Unfortunately, direct comparison of the values is problematic as different studies used different experimental conditions (e.g. intracellular solutions, temperature, culture *vs.* acute slice) and the recordings were obtained from animals of distinct species and at distinct stages of postnatal development. Furthermore, most central neurones express several $GABA_A$ receptor subtypes with largely unknown subunit composition, making the identification of 'kinetic fingerprints' of distinct types of synaptic $GABA_A$ receptor almost impossible.

In order to investigate the role of subunit composition in $GABA_A$ receptor kinetics, several studies have used ultrafast

GABA applications to outside-out patches pulled from cell lines transfected with recombinant receptors of known subunit composition. It has been convincingly demonstrated that $\alpha1\beta2\gamma2$ receptors have a sixfold faster deactivation rate than $\alpha2\beta1\gamma2$ receptors ($\tau_w \approx 18$ ms *vs.* $\tau_w \approx 80$ ms, respectively; Lavoie *et al.* 1997; McClellan & Twyman, 1999). Similarly, receptors with $\alpha6\beta2\gamma2$ subunit composition have a much slower deactivation rate than $\alpha1\beta2\gamma2$ receptors ($\tau_w \approx 70$ ms *vs.* $\tau_w \approx 160$ ms, respectively; Tia *et al.* 1996). These results indicate the importance of the subunit composition for shaping the kinetics of synaptic currents. However, as noted by several studies (Puia *et al.* 1994; Jones & Westbrook, 1995; Mozrzymas *et al.* 1999) the decay kinetics of the currents in excised patches are always slower than those of mIPSCs, making it difficult to directly compare the kinetics of patch currents and mIPSCs. Indeed, the above-mentioned deactivation time courses for the $\alpha1\beta x\gamma2$ receptors measured in patches (Tia *et al.* 1996; McClellan & Twyman, 1999) are much slower than our values of mIPSC decay in $\alpha1\beta2\gamma2$ receptor-expressing cerebellar interneurones ($\tau_w \approx 4$ ms) recorded at 32 °C, and still slower than mIPSC decays recorded in stellate cells at room temperature ($\tau_w \approx 9$ ms; Nusser *et al.* 1997).

In the present study, we have recorded mIPSCs from two different cell types expressing distinct $GABA_A$ receptor subtypes under identical experimental conditions (e.g. same temperature, solutions, age of animals, preparation of slices, etc.), allowing the direct comparison of IPSC decay kinetics. Cerebellar stellate/basket cells express only the $\alpha1$, $\beta2$ and $\gamma2$ subunits (Persohn *et al.* 1992; Nusser *et al.* 1999), very probably resulting in a single $GABA_A$ receptor subtype with $\alpha1\beta2\gamma2$ subunit composition. In contrast, olfactory bulb granule cells express high levels of $\alpha2$, $\alpha5$, $\beta3$, $\gamma2$ and δ subunits, which are likely to form $GABA_A$ receptors with $\alpha2\beta3\gamma2$, $\alpha5\beta3\gamma2$ and $\alpha x\beta3\delta$ subunit composition (McKernan & Whiting, 1996; Barnard *et al.* 1998). The contrasting difference in the kinetics of $mIPSC_{FR}$ recorded in olfactory bulb granule cells ($\tau_w = 15{\cdot}8$ ms) compared to mIPSCs in cerebellar interneurones ($\tau_w = 4{\cdot}2$ ms) indicates that the subunit composition plays an essential role in determining the decay kinetics of synaptic currents (Puia *et al.* 1994). Furthermore, the identification of two distinct mIPSCs in olfactory granule cells is in good agreement with the presence of more than one $GABA_A$ receptor subtype in these cells. If the δ subunit-containing receptors of the olfactory granule cells are also exclusively present extrasynaptically like in cerebellar granule cells (Nusser *et al.* 1998), then the segregation of $\alpha2\beta3\gamma2$ and $\alpha5\beta3\gamma2$ receptors to distinct synapses could explain the different kinetics of $mIPSC_{FR}$ and $mIPSC_{SR}$. Indeed, a recent immunocytochemical study with $\alpha2$ and $\alpha5$ subunit-selective antibodies revealed a differential distribution of these two α subunits in olfactory granule cells (Fritschy *et al.* 1998). Assuming that dendritic filtering is responsible for the slower rise times and smaller amplitudes of $mIPSC_{SR}$ compared to the fast rising currents, a faster decay time course of $mIPSC_{SR}$ than of $mIPSC_{FR}$ is predicted at their respective sites of origin. Thus, our data are consistent with $\alpha2\beta3\gamma2$ and $\alpha5\beta3\gamma2$ receptors generating synaptic currents with distinct decay kinetics that may be resolved by future pharmacological experiments. It has been shown that the effect of the benzodiazepine agonist zolpidem on $GABA_A$ receptors depends on the subunit composition. Namely, K_i values of zolpidem for displacing Ro-1788 from $GABA_A$ receptors with $\alpha2\beta3\gamma2$ and $\alpha5\beta3\gamma2$ subunit compositions are approximately 450 and 15 000 nM, respectively (Pritchett *et al.* 1990). In a recently completed study, we have found that the decay time courses of both $mIPSC_{FR}$ and $mIPSC_{SR}$ are prolonged to a similar extent by 20 μM zolpidem, indicating that $GABA_A$ receptors underlying both types of IPSCs are benzodiazepine sensitive (N. Hajos, Z. Nusser, E. A. Rancz, T. F. Freund & I. Mody, unpublished observations). Future pharmacological experiments with lower concentrations of zolpidem will have to be carried out in order to further dissect the $GABA_A$ receptor subtypes responsible for the two types of mIPSCs in olfactory granule cells.

The effect of PKA-dependent phosphorylation on synaptic currents depends on the subunit composition of the receptors

Several studies have investigated how the subunit composition of $GABA_A$ receptors determines the functional consequences of Ser/Thr phosphorylation (Kellenberger *et al.* 1992; Moss *et al.* 1992; Leidenheimer, 1996; McDonald *et al.* 1998). The results of the early studies showed either a reduction (Porter *et al.* 1990; Moss *et al.* 1992) or an enhancement (Kano & Konnerth, 1992; Kapur & Macdonald, 1996) of GABA-activated whole-cell currents by PKA-dependent phosphorylation. In an elegant study, McDonald *et al.* (1998) identified a critical role for the β subunits in determining the functional consequences of PKA-dependent phosphorylation of $GABA_A$ receptors. Phosphorylation of $\beta1$ subunit-containing recombinant $GABA_A$ receptors expressed in HEK 293 cells decreased, whereas phosphorylation of $\beta3$ subunit-containing receptors enhanced, GABA-activated currents. Furthermore, receptors containing the $\beta2$-type β subunit were not affected by PKA. As these functional experiments were carried out under 'equilibrium conditions', which are unlike those present at synapses, we wanted to determine how PKA-dependent phosphorylation regulates synaptic $GABA_A$ receptor function in cells expressing distinct β subunit variants. Our results from the $\beta3$ subunit-expressing olfactory granule cells, showing an increase in mIPSC amplitude, are in good agreement with the results of McDonald *et al.* (1998). These results, however, are in contrast to those of a recent study examining the effect of PKA-mediated phosphorylation on GABA-evoked whole-cell currents recorded from olfactory granule cells (Brunig *et al.* 1999). Differences between our experimental conditions and those of Brunig *et al.* (1999), which may explain this discrepancy, include the use of acute slices from P17–P25 mice *vs.* 5- to 7-day-old cultured neurones, recording at 32 °C *vs.* room temperature and examining the effect of PKA on mIPSCs *vs.* GABA-evoked whole-cell currents.

It has been demonstrated that PKA-dependent phosphorylation of GluR6 subunit-containing kainate receptors modifies the open probability (P_o) of the receptors (Traynelis & Wahl, 1997). If a similar mechanism applies for $GABA_A$ receptors, our results in olfactory granule cells can be explained by an increase in P_o of the $GABA_A$ receptors after PKA-mediated phosphorylation. Similarly, the observed reduction of mIPSC amplitude after phosphorylation by PKA in hippocampal CA1 pyramidal cells (Poisbeau *et al.* 1999) could also be due to changes in the P_o of the receptors, but perhaps through an effect on $GABA_A$ receptors with dissimilar subunit composition. Alternatively, a change in the single channel conductance may also result from phosphorylation as demonstrated for the glutamate receptors (Derkach *et al.* 1999). As $GABA_A$ receptors can change their main conductance levels in the presence of benzodiazepines (Eghbali *et al.* 1997), this possibility needs to be further investigated for the phosphorylation-dependent regulation of synaptic $GABA_A$ receptors.

We also detected an increase in the charge transferred by synaptic currents in the $\alpha1\beta2\gamma2$-containing cerebellar stellate/basket cells after PKA phosphorylation, but through a completely different mechanism. As there was no change in the peak amplitude, an alteration in P_o can be ruled out. It is more likely that the prolongation of the decay is due to an increase of the microscopic unbinding rate of the receptors as both the first and second exponential components were prolonged by a similar extent. This result is inconsistent with the finding of McDonald *et al.* (1998), who did not observe a direct phosphorylation of $\beta2$ subunit-containing receptors. Our result is also at odds with that of Kano & Konnerth (1992), who described an increase in the amplitude of mIPSCs recorded in cerebellar Purkinje cells, which very probably express the same subunits of the $GABA_A$ receptors as stellate and basket cells (Persohn *et al.* 1992). However, it should be noted that changes in synaptic currents do not provide evidence for the direct phosphorylation of $GABA_A$ receptors. Proteins associated with synaptic receptors (Essricht *et al.* 1998; Wang *et al.* 1999) could also be substrates of PKA and may cause a change in the postsynaptic current. Thus, a differential distribution of $GABA_A$-associated proteins in stellate/basket *vs.* Purkinje cells could explain the discrepancy observed in the regulation of mIPSCs by PKA in these cells.

The control of the phosphorylation of mIPSCs by protein phosphatases is cell-type dependent

Several studies have demonstrated that $GABA_A$ receptors can be phosphorylated by cAMP, cGMP, Ca^{2+}–phospholipid-dependent kinases, Ca^{2+}–calmodulin-dependent protein kinase II and protein tyrosine kinases (reviewed by Moss & Smart, 1996). However, much less is known about whether such phosphorylation indeed occurs in nerve cells at synapses where $GABA_A$ receptors are concentrated (Fritschy & Mohler, 1995; Nusser *et al.* 1995, 1996, 1997). To investigate whether a basic phosphorylation–dephosphorylation cycle regulates synaptic $GABA_A$ receptor function, we intracellularly applied a membrane-impermeant PP1/2A inhibitor (microcystin). In cerebellar stellate/basket cells, microcystin prolonged the decay time course of mIPSCs, demonstrating that a constantly active PP1/2A dephosphorylated the $GABA_A$ receptors or some related proteins. As the co-application of PKA-I with microcystin counteracted the effect of microcystin on the synaptic current decays, we identified the kinase involved in the phosphorylation process as PKA. Furthermore, as application of PKA-I alone did not result in an acceleration of mIPSC decay, the phosphorylation state of the proteins involved appears to be overwhelmingly controlled by a strong PP1/2A activity. Thus, under control conditions, the rate of dephosphorylation of these proteins is probably faster than their phosphorylation rate. An almost identical result has been observed in hippocampal CA1 pyramidal cells, where a strong phosphatase (PP1/2A) activity also controls the phosphorylation–dephosphorylation processes (Poisbeau *et al.* 1999). However, we cannot generalise from these results to every cell type as blocking the phosphatase activity did not change any of the mIPSC parameters in dentate gyrus and olfactory bulb granule cells and in hippocampal pyramidal cells in culture (Jones & Westbrook, 1997; Poisbeau *et al.* 1999; present study). Thus, it needs to be specifically analysed in every cell type of interest whether a strong phosphatase activity controls the phosphorylation–dephosphorylation state of synaptic $GABA_A$ receptor function.

Of the two cell types where continuous phosphorylation–dephosphorylation processes control the PKA-mediated regulation of synaptic $GABA_A$ receptor function, hippocampal CA1 pyramidal cells seem to become more excitable upon the activation of processes that shift the phosphorylation–dephosphorylation balance towards a more phosphorylated state (Jones & Westbrook, 1997; Poisbeau *et al.* 1999). Interestingly, Jones & Westbrook (1997) found a shortening of the decay time course of IPSCs in cultured hippocampal pyramidal cells after blocking calcineurin activity, whereas Poisbeau *et al.* (1999) observed a decrease in the peak amplitude of the synaptic currents following the inhibition of PP1/2A. Despite these differences, the charge transferred by the synaptic currents decreased after inhibition of phosphatase activity. In contrast, an equivalent event leading to the prevalence of phosphorylation will result in an overall decrease in the excitability of cerebellar interneurones. These seemingly opposing effects may work in harmony to achieve the same outcome on the network activity. Pyramidal cells are the principal cells in the CA1 area and are glutamatergic, whereas stellate and basket cells are the GABAergic inhibitory interneurones of the molecular layer of the cerebellar cortex. Thus, a PKA-dependent reduction of the inhibition of pyramidal cells will result in an increase in the overall excitability of the hippocampal CA1 area. A similar increase in the excitability of the cerebellar molecular layer is predicted upon an enhanced phosphorylation of synaptic $GABA_A$ receptors in GABAergic interneurones. It will be interesting to see

whether a continuous phosphorylation–dephosphorylation cycle is also responsible for the regulation of synaptic $GABA_A$ receptor function in hippocampal GABAergic interneurones. A PKA-mediated phosphorylation may result in an increased synaptic inhibition in these cells, leading to an elevated excitability of the whole network following an enhanced phosphorylation in each of the diverse elements of the neural network.

Auger, C. & Marty, A. (1997). Heterogeneity of functional synaptic parameters among single release sites. *Neuron* **19**, 139–150.

Barnard, E. A., Skolnick, P., Olsen, R. W., Mohler, H., Sieghart, W., Biggio, G., Braestrup, C., Bateson, A. N. & Langer, S. Z. (1998). International union of pharmacology. XV. Subtypes of γ-aminobutyric $acid_A$ receptors: classification on the basis of subunit structure and receptor function. *Pharmacological Reviews* **50**, 291–313.

Brickley, S. G., Cull-Candy, S. G. & Farrant, M. (1999). Single-channel properties of synaptic and extrasynaptic $GABA_A$ receptors suggest differential targeting of receptor subtypes. *Journal of Neuroscience* **19**, 2960–2973.

Browning, M. D., Bureau, M., Dudek, E. M. & Olsen, R. W. (1990). Protein kinase C and cAMP-dependent protein kinase phosphorylate the β subunit of the purified γ-aminobutyric acid A receptor. *Proceedings of the National Academy of Sciences of the USA* **87**, 1315–1318.

Brunig, I., Sommer, M., Hatt, H. & Bormann, J. (1999). Dopamine receptor subtypes modulate olfactory bulb γ-aminobutyric acid type A receptors. *Proceedings of the National Academy of Sciences of the USA* **96**, 2456–2460.

Clements, J. D. (1996). Transmitter timecourse in the synaptic cleft: its role in central synaptic function. *Trends in Neurosciences* **19**, 163–171.

Derkach, V., Barria, A. & Soderling, T. R. (1999). Ca^{2+}/calmodulin-kinase II enhances channel conductance of α-amino-3-hydroxy-5-methyl-4-isoxazolepropionate type glutamate receptors. *Proceedings of the National Academy of Sciences of the USA* **96**, 3269–3274.

Edwards, F. A., Konnerth, A. & Sakmann, B. (1990). Quantal analysis of inhibitory synaptic transmission in the dentate gyrus of rat hippocampal slices: a patch-clamp study. *Journal of Physiology* **430**, 213–249.

Eghbali, M., Curmi, J. P., Birnir, B. & Gage, P. W. (1997). Hippocampal $GABA_A$ channel conductance increased by diazepam. *Nature* **388**, 71–75.

Essricht, C., Lorez, M., Benson, J. A., Fritschy, J.-M. & Luscher, B. (1998). Postsynaptic clustering of major $GABA_A$ receptor subtypes requires the γ2 subunit and gephyrin. *Nature Neuroscience* **1**, 563–571.

Freund, T. F. & Buzsaki, G. (1996). Interneurons of the hippocampus. *Hippocampus* **6**, 347–470.

Fritschy, J.-M., Johnson, D. K., Mohler, H. & Rudolph, U. (1998). Independent assembly and subcellular targeting of $GABA_A$-receptor subtypes demonstrated in mouse hippocampal and olfactory neurons in vivo. *Neuroscience Letters* **249**, 99–102.

Fritschy, J.-M. & Mohler, H. (1995). $GABA_A$-receptor heterogeneity in the adult rat brain: differential regional and cellular distribution of seven major subunits. *Journal of Comparative Neurology* **359**, 154–194.

Hanley, J. G., Koulen, P., Bedford, F., Gordon-Weeks, P. R. & Moss, S. J. (1999). The protein MAP-1B links $GABA_C$ receptors to the cytoskeleton at retinal synapses. *Nature* **397**, 66–69.

Jechlinger, M., Pelz, R., Tretter, V., Klausberger, T. & Sieghart, W. (1998). Subunit composition and quantitative importance of hetero-oligomeric receptors: $GABA_A$ receptors containing α6 subunits. *Journal of Neuroscience* **18**, 2449–2457.

Jones, M. V. & Westbrook, G. L. (1995). Desensitized states prolong $GABA_A$ channel responses to brief agonist pulses. *Neuron* **15**, 181–191.

Jones, M. V. & Westbrook, G. L. (1996). The impact of receptor desensitization on fast synaptic transmisson. *Trends in Neurosciences* **19**, 96–101.

Jones, M. V. & Westbrook, G. L. (1997). Shaping of IPSCs by endogenous calcineurin activity. *Journal of Neuroscience* **17**, 7626–7633.

Kano, M. & Konnerth, A. (1992). Potentiation of GABA-mediated currents by cAMP-dependent protein kinase. *NeuroReport* **3**, 563–566.

Kapur, J. & Macdonald, R. L. (1996). Cyclic AMP-dependent protein kinase enhances hippocampal dentate granule cell $GABA_A$ receptor currents. *Journal of Neurophysiology* **76**, 2626–2634.

Kellenberger, S., Malherbe, P. & Sigel, E. (1992). Function of the $\alpha1\beta2\gamma2S$ γ-aminobutyric acid type A receptor is modulated by protein kinase-C via multiple phosphorylation sites. *Journal of Biological Chemistry* **267**, 25660–25663.

Lavoie, A. M., Tingey, J. J., Harrison, N. L., Pritchett, D. B. & Twyman, R. E. (1997). Activation and deactivation rates of recombinant $GABA_A$ receptor channels are dependent on α-subunit isoform. *Biophysical Journal* **73**, 2518–2526.

Lavoie, A. M. & Twyman, R. E. (1996). Direct evidence for diazepam modulation of $GABA_A$ receptor microscopic affinity. *Neuropharmacology* **35**, 1383–1392.

Leidenheimer, N. J. (1996). Effect of PKG activation on recombinant $GABA_A$ receptors. *Molecular Brain Research* **42**, 131–134.

Llano, I. & Gerschenfeld, H. M. (1993). Inhibitory synaptic currents in stellate cells of rat cerebellar slices. *Journal of Physiology* **468**, 177–200.

McClellan, A. M. & Twyman, R. E. (1999). Receptor system response kinetics reveal functional subtypes of native murine and recombinant human $GABA_A$ receptors. *Journal of Physiology* **515**, 711–727.

McDonald, B. J., Amato, A., Connolly, C. N., Benke, D., Moss, S. J. & Smart, T. G. (1998). Adjacent phosphorylation sites on $GABA_A$ receptor β subunits determine regulation by cAMP-dependent protein kinase. *Nature Neuroscience* **1**, 23–28.

Macdonald, R. L. & Olsen, R. W. (1994). $GABA_A$ receptor channels. *Annual Review of Neuroscience* **17**, 569–602.

McKernan, R. M. & Whiting, P. J. (1996). Which $GABA_A$-receptor subtypes really occur in the brain? *Trends in Neurosciences* **19**, 139–143.

Moss, S. J. & Smart, T. G. (1996). Modulation of amino acid-gated ion channels by protein phosphorylation. *International Review of Neurobiology* **39**, 1–52.

Moss, S. J., Smart, T. G., Blackstone, C. D. & Huganir, R. L. (1992). Functional modulation of $GABA_A$ receptors by cAMP-dependent protein phosphorylation. *Science* **257**, 661–665.

Mozrzymas, J. W., Barberis, A., Michalak, K. & Cherubini, E. (1999). Chlorpromazine inhibits miniature GABAergic currents by reducing the binding and by increasing the unbinding rate of $GABA_A$ receptors. *Journal of Neuroscience* **19**, 2474–2488.

Nusser, Z., Ahmad, Z., Tretter, V., Fuchs, K., Wisden, W., Sieghart, W. & Somogyi, P. (1999). Alterations in the expression of $GABA_A$ receptor subunits in cerebellar granule cells after the disruption of the α6 subunit gene. *European Journal of Neuroscience* **11**, 1685–1697.

Nusser, Z., Cull-Candy, S. G. & Farrant, M. (1997). Differences in synaptic $GABA_A$ receptor number underlie variation in GABA mini amplitude. *Neuron* **19**, 697–709.

Nusser, Z., Roberts, J. D. B., Baude, A., Richards, J. G., Sieghart, W. & Somogyi, P. (1995). Immunocytochemical localization of the α1 and β2/3 subunits of the $GABA_A$ receptor in relation to specific GABAergic synapses in the dentate gyrus. *European Journal of Neuroscience* **7**, 630–646.

Nusser, Z., Sieghart, W., Benke, D., Fritschy, J.-M. & Somogyi, P. (1996). Differential synaptic localization of two major γ-aminobutyric acid type A receptor α subunits on hippocampal pyramidal cells. *Proceedings of the National Academy of Sciences of the USA* **93**, 11939–11944.

Nusser, Z., Sieghart, W. & Somogyi, P. (1998). Segregation of different $GABA_A$ receptors to synaptic and extrasynaptic membranes of cerebellar granule cells. *Journal of Neuroscience* **18**, 1693–1703.

Otis, T. S. & Mody, I. (1992). Modulation of decay kinetics and frequency of GABA-receptor-mediated spontaneous inhibitory postsynaptic currents in hippocampal neurons. *Neuroscience* **49**, 13–32.

Perrais, D. & Ropert, N. (1999). Effect of zolpidem on miniature IPSCs and occupancy of postsynaptic $GABA_A$ receptors in central synapses. *Journal of Neuroscience* **19**, 578–588.

Persohn, E., Malherbe, P. & Richards, J. G. (1992). Comparative molecular neuroanatomy of cloned $GABA_A$ receptor subunits in the rat CNS. *Journal of Comparative Neurology* **326**, 193–216.

Poisbeau, P., Cheney, M. C., Browning, M. D. & Mody, I. (1999). Modulation of synaptic $GABA_A$ receptor function by PKA and PKC in adult hippocampal neurons. *Journal of Neuroscience* **19**, 674–683.

Porter, N. M., Twyman, R. E., Uhler, M. D. & Macdonald, R. L. (1990). Cyclic AMP-dependent protein kinase decreases $GABA_A$ receptor current in mouse spinal neurons. *Neuron* **5**, 789–796.

Pritchett, D. B. & Seeburg, P. H. (1990). γ-Aminobutyric acidA receptor α5-subunit creates novel type II benzodiazepine receptor pharmacology. *Journal of Neurochemistry* **54**, 1802–1804.

Puia, G., Costa, E. & Vicini, S. (1994). Functional diversity of GABA-activated Cl^- currents in Purkinje versus granule neurons in rat cerebellar slices. *Neuron* **12**, 117–126.

Sieghart, W. (1995). Structure and pharmacology of γ-aminobutyric $acid_A$ receptor subtypes. *Pharmacological Reviews* **47**, 181–234.

Slany, A., Zezula, J., Tretter, V. & Sieghart, W. (1995). Rat β3 subunits expressed in human embryonic kidney 293 cells form high affinity [^{35}S]t-butylbicyclophosphorothionate binding sites modulated by several allosteric ligands of γ-aminobutyric acid type A receptors. *Molecular Pharmacology* **48**, 385–391.

Somogyi, P., Takagi, H., Richards, J. G. & Mohler, H. (1989). Subcellular localization of benzodiazepine/$GABA_A$ receptors in the cerebellum of rat, cat, and monkey using monoclonal antibodies. *Journal of Neuroscience* **9**, 2197–2209.

Sperk, G., Schwarzer, C., Tsunashima, K., Fuchs, K. & Sieghart, W. (1997). $GABA_A$ receptor subunits in the rat hippocampus I: immunocytochemical distribution of 13 subunits. *Neuroscience* **80**, 987–1000.

Tia, S., Wang, J. F., Kotchabhakdi, N. & Vicini, S. (1996). Distinct deactivation and desensitization kinetics of recombinant $GABA_A$ receptors. *Neuropharmacology* **35**, 1375–1382.

Traynelis, S. F. & Wahl, P. (1997). Control of rat GluR6 glutamate receptor open probability by protein kinase A and calcineurin. *Journal of Physiology* **503**, 513–531.

Wang, H., Bedford, F. K., Brandon, N. J., Moss, S. J. & Olsen, R. W. (1999). $GABA_A$-receptor-associated protein links $GABA_A$ receptors and the cytoskeleton. *Nature* **397**, 69–72.

Wisden, W., Laurie, D. J., Monyer, H. & Seeburg, P. H. (1992). The distribution of 13 $GABA_A$ receptor subunit mRNAs in the rat brain. I. Telencephalon, diencephalon, mesencephalon. *Journal of Neuroscience* **12**, 1040–1062.

Acknowledgements

We would like to thank Dr M. D. Browning for kindly providing the constitutively active catalytic subunit of PKA and PKA inhibitory peptide. This work was supported by a NINDS grant (NS 30549) and the Coelho Endowment to I.M.; a Wellcome International Prize Travelling Research Fellowship to Z.N.; and a European Commission Shared Cost RTD Programme Grant (no. BIO4CT96-0585) to W.S.

Corresponding author

Z. Nusser: Department of Neurology, UCLA School of Medicine, 710 Westwood Plaza, Los Angeles, CA 90095-1769, USA.

Email: nusser@ucla.edu